# *Ab initio* generation of binary alloy foams: the case of amorphous $Cu_{64}Zr_{36}$

Jonathan Galván  Ariel A. Valladares

Renela M. Valladares  Alexander Valladares

Materials Research Institute, UNAM

2nd International Electronic Conference on Materials, 2016

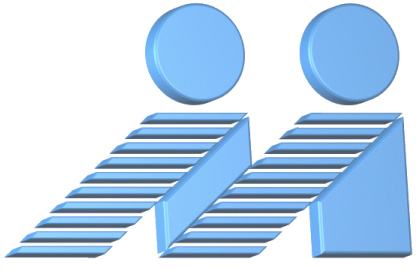

# Outline

# Background

# Experimental pore-making I

- Gas-generated foams
  - Bubbling gas into molten metals
  - Gas releasing from chemical-breaking at high temperatures when adding powders to molten metals
  - H can be dissolved in many liquid metals; upon solidification, H is rejected
- Template porous
  - Casting into a mold
  - Powder deposition
  - Decomposition
  - Electrodeposition

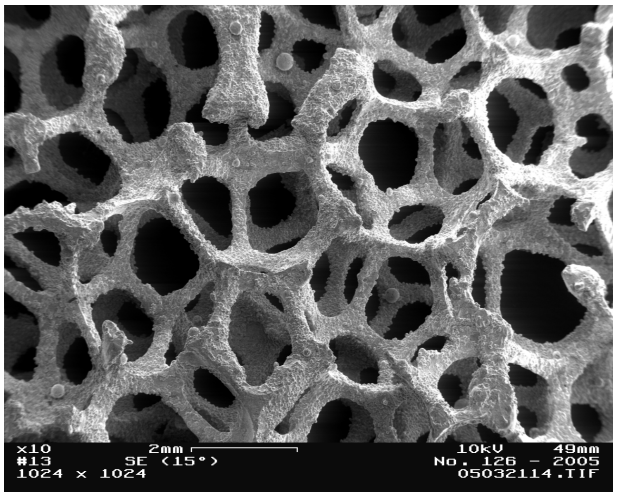

# Experimental pore-making II

- Individual elements assembly
  - Spray forming
  - Sintering powders, wires or hollow spheres
  - Selective sintering
- Removable 2nd phase
  - Casting into space holders
  - Sintering with space holders
  - Replication
  - Dealloying (small scale pores $\sim$ several nm)

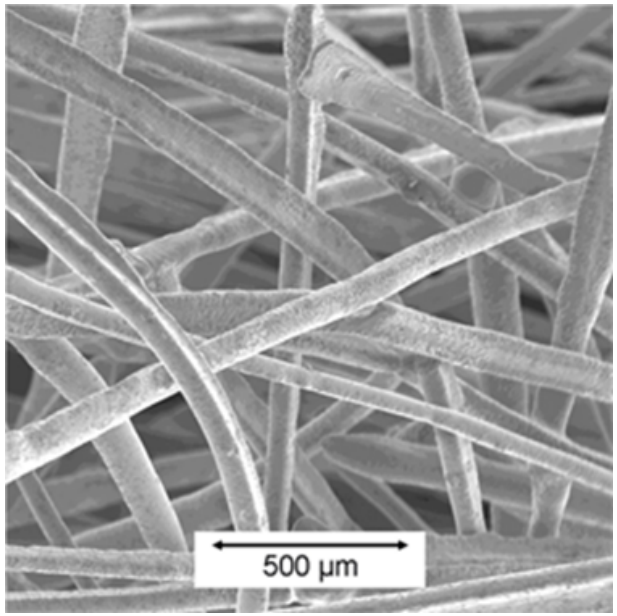


Clyne, University of Cambridge (2010)

# Early works

- The first successful method to create a bulk metallic glass foam was reported by Schroers *et al.* $Pd_{43}Cu_{27}Ni_{10}P_{20}$ with pores of 200-1000 $\mu$m
- Brothers and Dunand reported the foaming of a Zr-based alloy by rapid quenching in 2004: $Zr_{57}Nb_5Cu_{15.4}Ni_{12.6}Al_{10}$ with pore sizes of 25-50 $\mu$m
- Successive experimental works were focused on multicomponent alloys: $Ni_{59}Zr_{20}Ti_{16}Si_2Sn_3$, $Fe_{48}Cr_{15}Mo_{14}Y_2C_{15}B_6$, and $Mg_{60}Cu_{21}Ag_7Gd_{12}$

Schroers *et al.*, App. Phys. Lett. 82, 370 (2003)
Brothers, Dunand, App. Phys. Lett 84, 1108 (2004)
Lee, Sordelet, App. Phys. Lett. 89 (2006)
Demetreiou *et al.*, Scripta Mater. 57, 9 (2007)
Brothers *et al.*, J. App. Phys. 102, 023508 (2007)

# Porous materials from simulations

- Reconstructive approach:
  - The model structure is based on experimental reference data
  - Problem of uniqueness arises
  - Reverse Monte Carlo: energy determined by how well the structure reproduces empirical data, e.g., structure factor
- Mimetic approach
  - Mimics physical and chemical processes to generate the experimental sample
  - Monte Carlo or Molecular Dynamics are used to model the evolution of the structure from a starting state
  - Empirical or semi-empirical potentials have no transferability
- Pores are manually carved in the structure
- No *ab initio* approaches have been cited

Gelb, MRS Bull. 34, 592 (2009)

# Why amorphous porous metals?

# Bulk metallic glasses - Properties

- Lack of long range order
- Glass Forming Ability depends on contents
- Enhanced mechanical properties than other crystalline materials
- High viscosity
- Micro- and nano-size forming molds
- Catalysts
- High wear and corrosion resistance

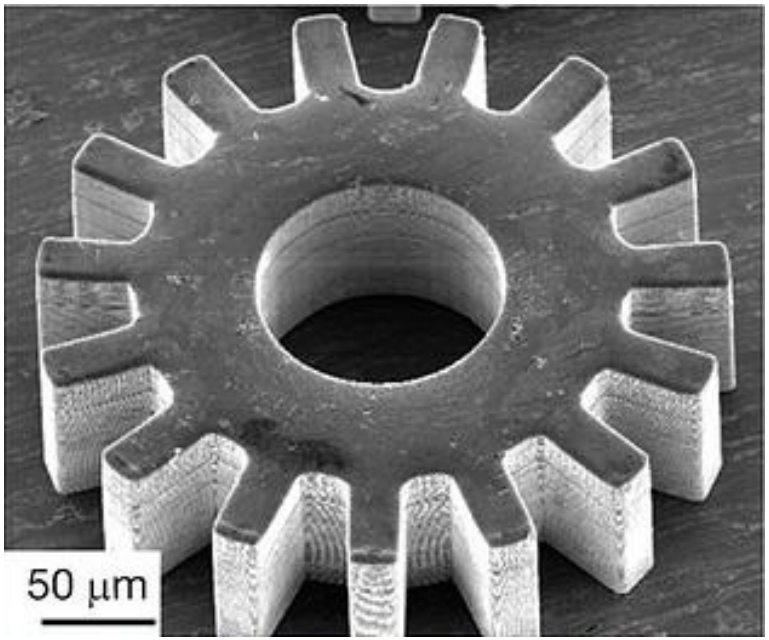


Kumar, Tang, Schroers, Nature 457, 868 (2009)

# Bulk metallic glasses - Drawbacks

- Lack of ductility
- Size-growth limit
- High brittleness
- Generation techniques are under development
- Higher serial production costs than crystalline counterparts

# Metallic foams and sponges - Properties

- Research dates back to early 1990s
- Improved mechanical properties under compression, bending and torsion
- Lightweight structures
- Impact/blast mitigation
- Fluid filters
- Gas storage

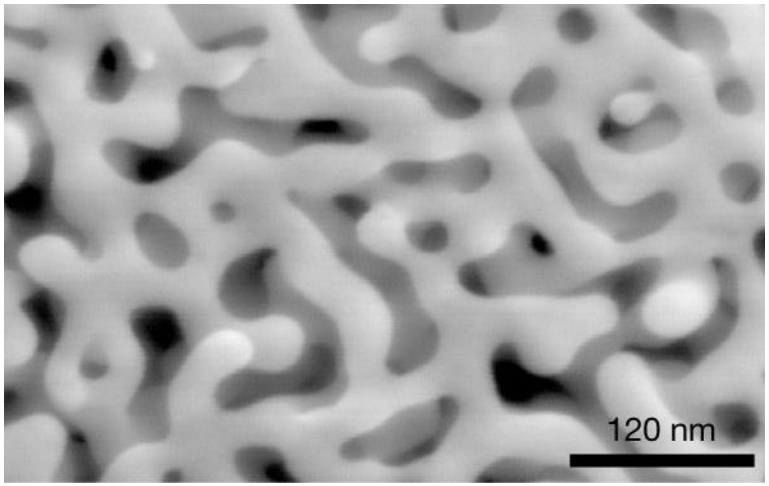


Erlebacher, Nature 410, 450 (2001)

# Metallic foams and sponges - Drawbacks

- Mechanical properties limited by the base alloys
- Difficult fabrication processes
- External phases while foaming due to blowing agents or solid placeholders
- Pore size control in the nano-regime

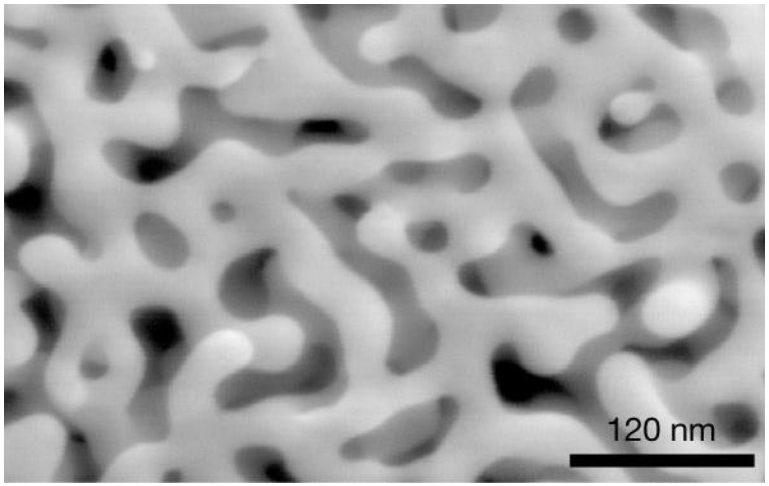


Erlebacher, Nature 410, 450 (2001)

# Amorphous porous alloys

- Combine both properties of amorphous metals and metallic foams
- Experimental procedures design becomes complex
- Computer simulation modeling is useful to predict properties: topological, electronic, vibrational, mechanical, etc.
- Brand-new research field $\sim$ 10 years

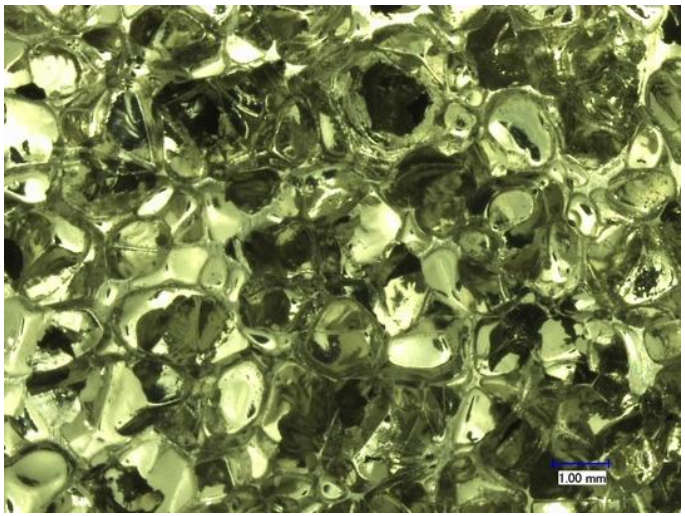

# Method

# The Expanding Lattice (EL) Method

The edge of the cubic cell is enlarged and the interatomic distances are proportionally increased. The volume increases and the density decreases as $l_2 = 2^{1/3} l_1$ for a 50 % of porosity.

- This approach has been applied to semiconductors and pure metals, such as: carbon, silicon, aluminum, copper and gold.
- Some properties as eDOS and vDOS have been calculated for amorphous nanoporous carbon which have agreed with other simulations and experimental data.
- Energetics of hydrogen adsorption have been calculated in amorphous nanoporous carbon and silicon.

Valladares *et al.*, Mater. Res. Soc. Symp. Proc. 971 (2007)
Valladares *et al.*, Mater. Res. Soc. Symp. Proc. 988 (2007)
Valladares *et al.*, Mater. Res. Soc. Symp. Proc. 1042 (2008)
Romero *et al.*, Materials 3, 467 (2010)
Santiago-Cortés *et al.*, J. Non-Cryst. Solids 358, 596 (2012)
Romero *et al.*, J. Non-Cryst. Solids 362, 14 (2013)

# The EL method in 108-atom $Cu_{64}Zr_{36}$

**From crystal**

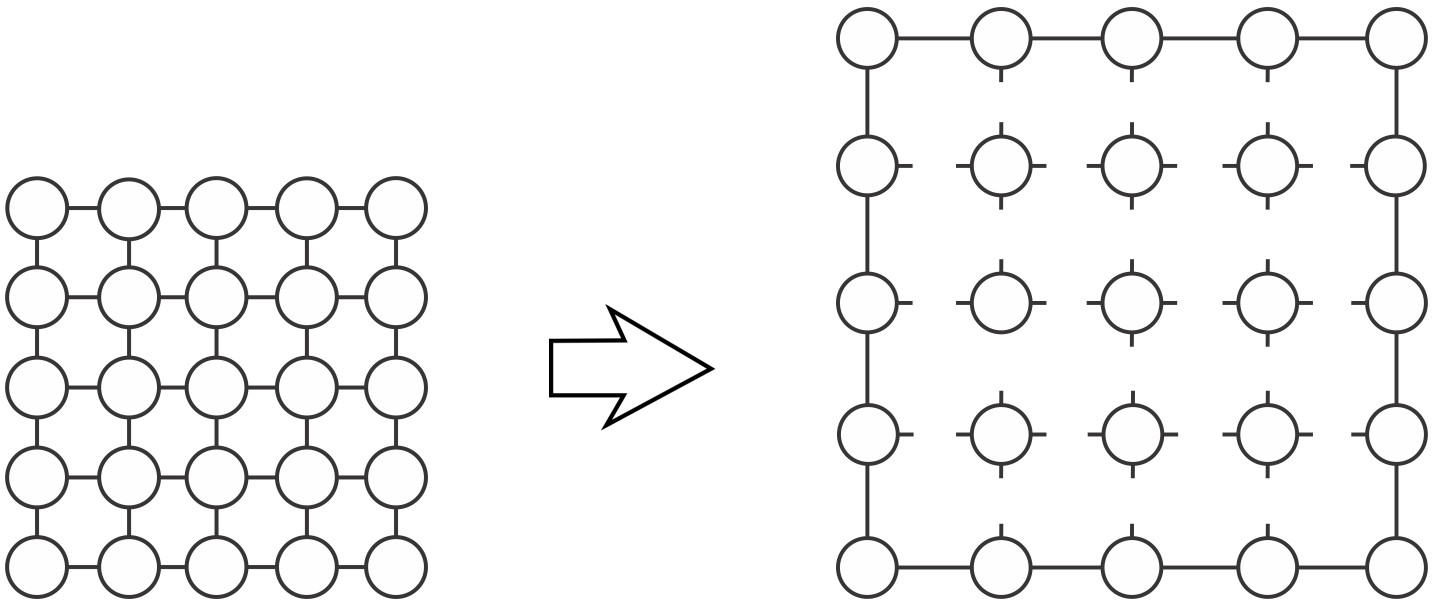

# The EL method in 108-atom $Cu_{64}Zr_{36}$

**From amorphous**

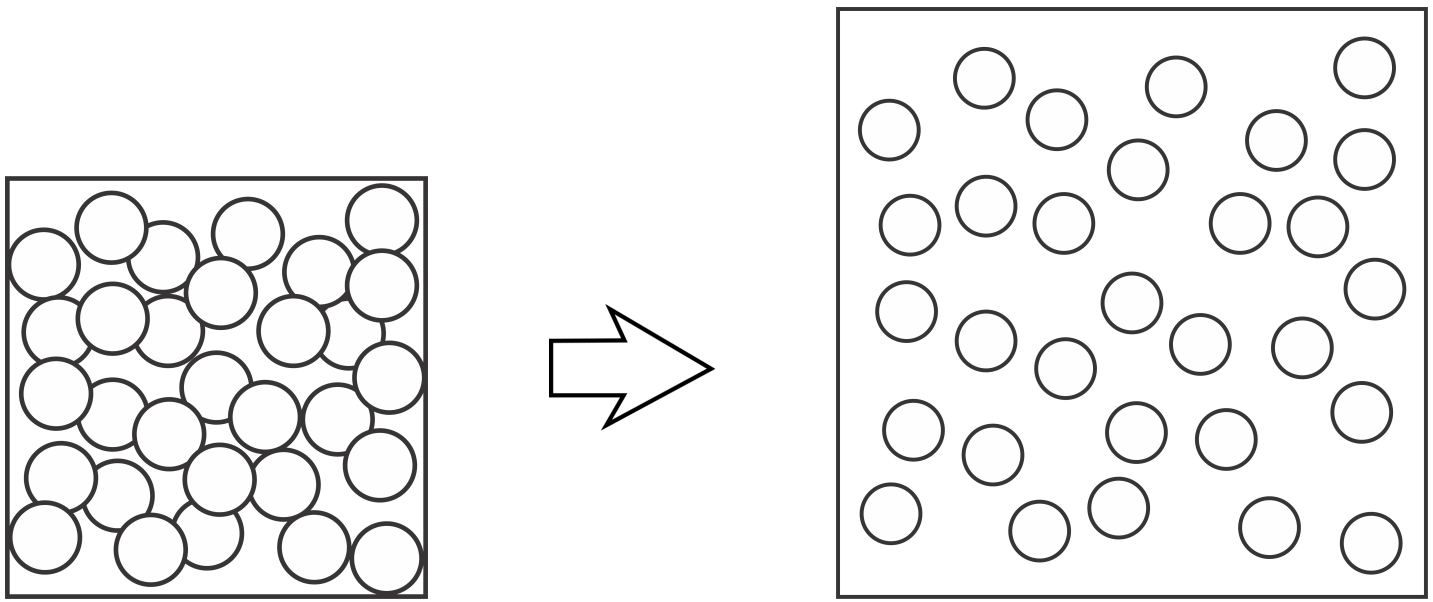

Valladares *et al.*, Materials 4 (2011)
Galván-Colín, *et al.*, Mater. Res. Soc. Symp. Proc. 1517 (2013)
Galván-Colín, *et al.*, Physica B 475 (2015)

## The Process

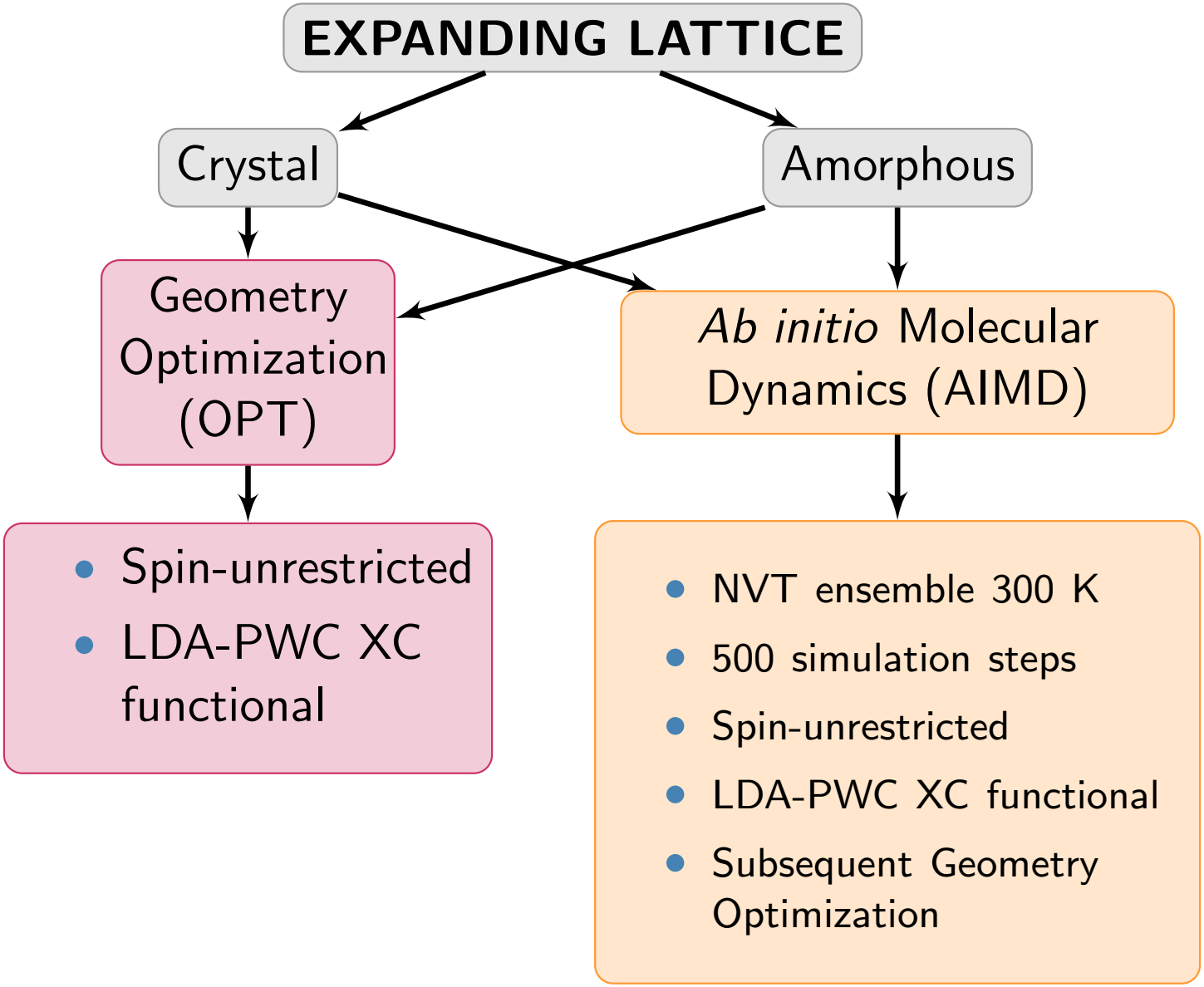
EXPANDING LATTICE
Crystal
Amorphous
Geometry Optimization (OPT)
Ab initio Molecular Dynamics (AIMD)
Spin-unrestricted
LDA-PWC XC functional
NVT ensemble 300 K
500 simulation steps
Spin-unrestricted
LDA-PWC XC functional
Subsequent Geometry Optimization

# Results

# OPT-generated ap-$Cu_{64}Zr_{36}$ structures

## From crystal

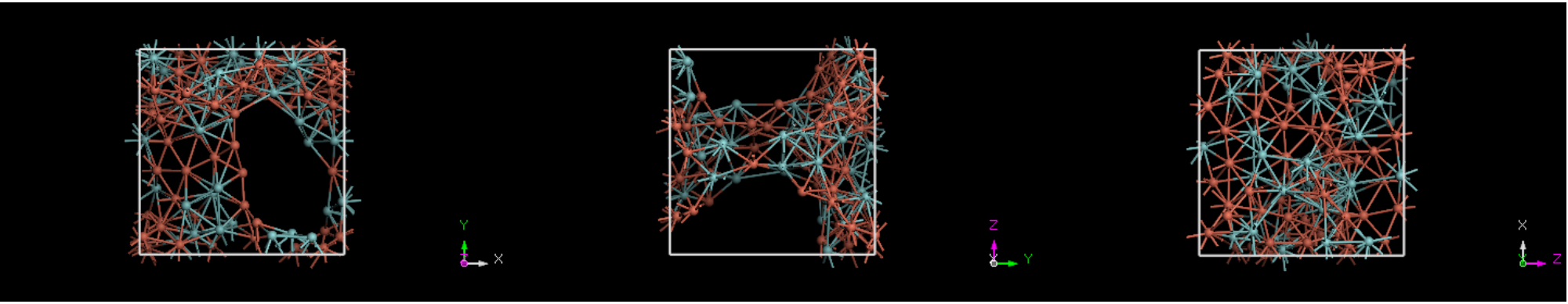

## From amorphous

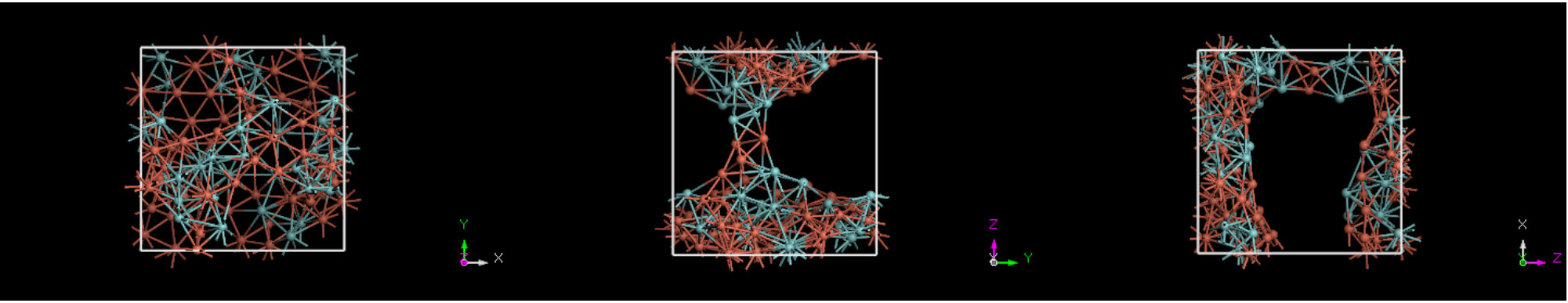

# AIMD-generated ap-$Cu_{64}Zr_{36}$ structures

## From crystal

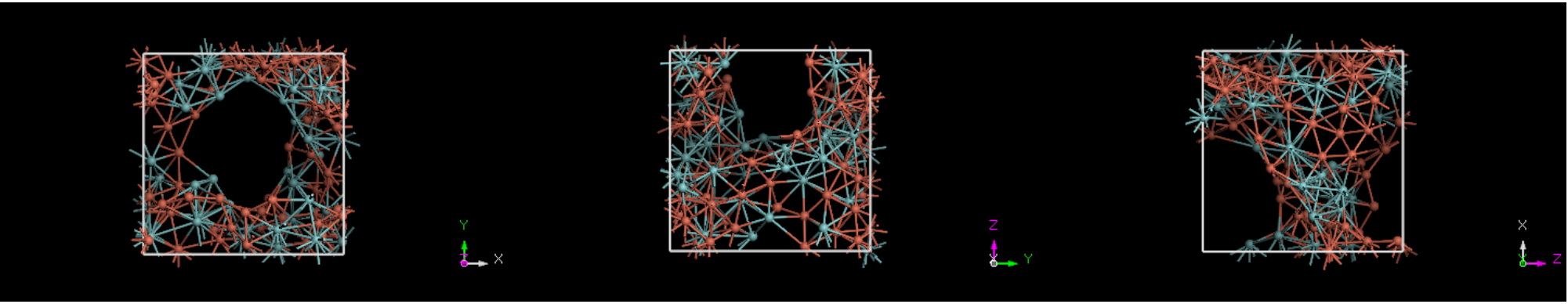

## From amorphous

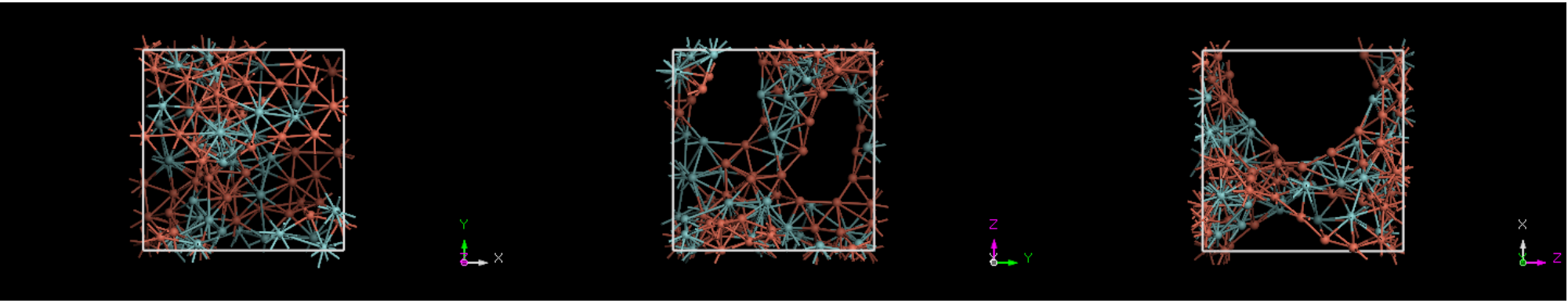

# ap-$Cu_{64}Zr_{36}$ Cu-Cu partials

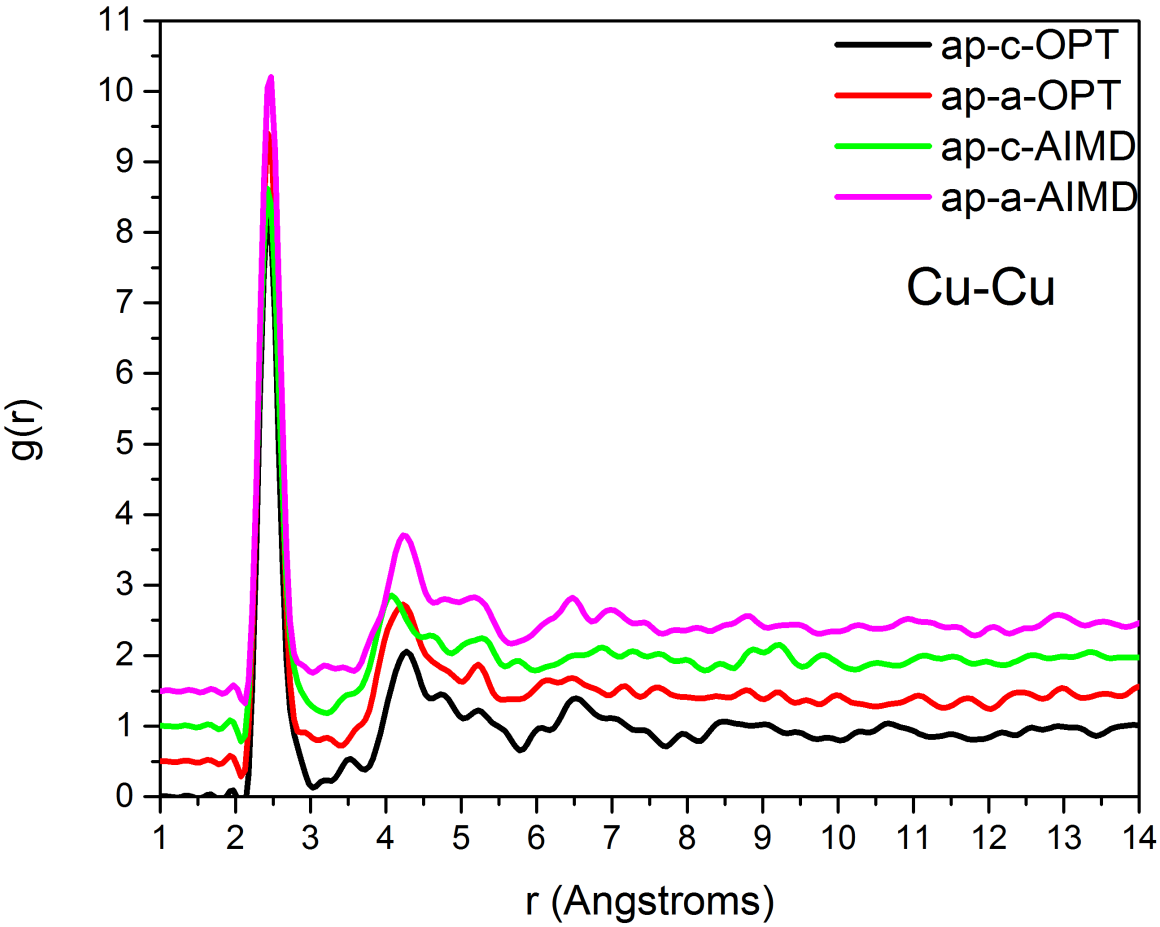

# ap-$Cu_{64}Zr_{36}$ Cu-Zr partials

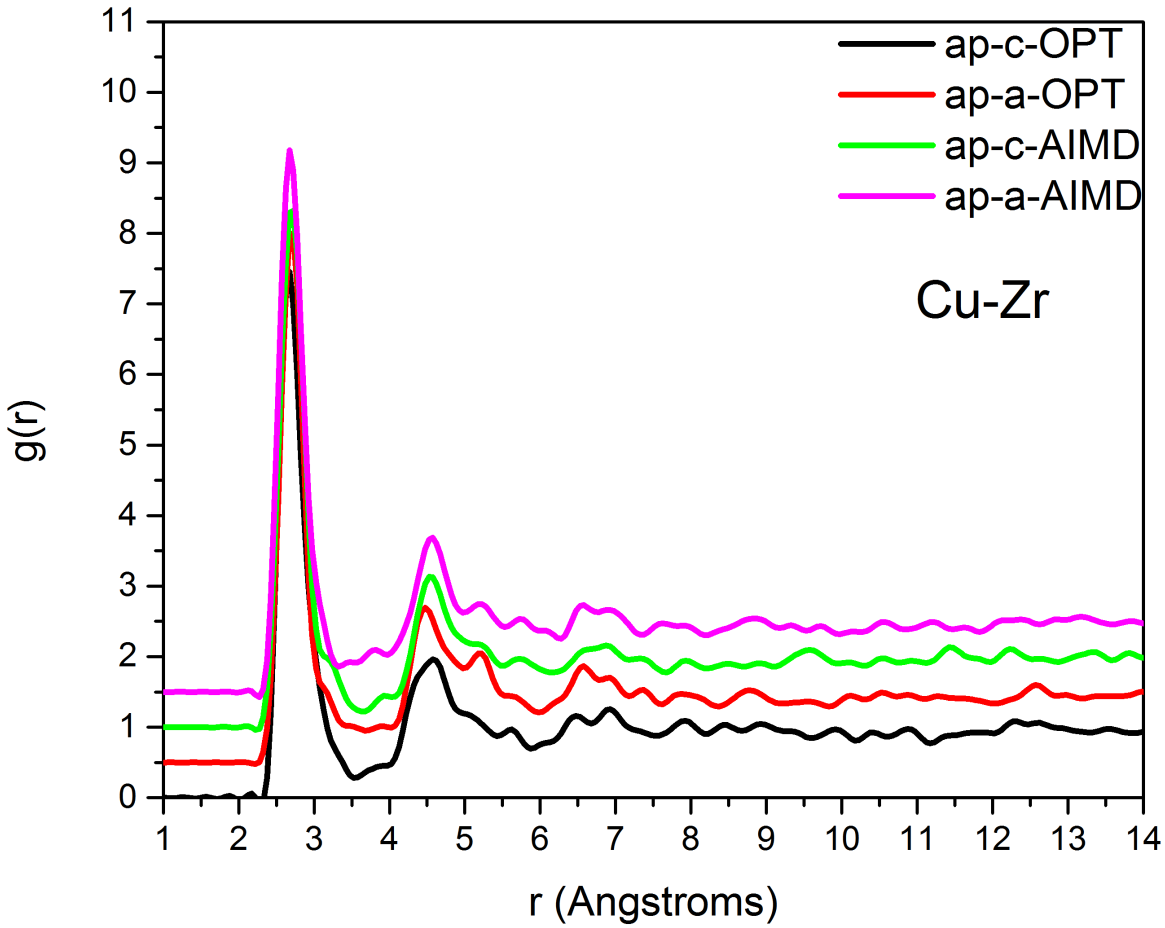

# ap-$Cu_{64}Zr_{36}$ Zr-Zr partials

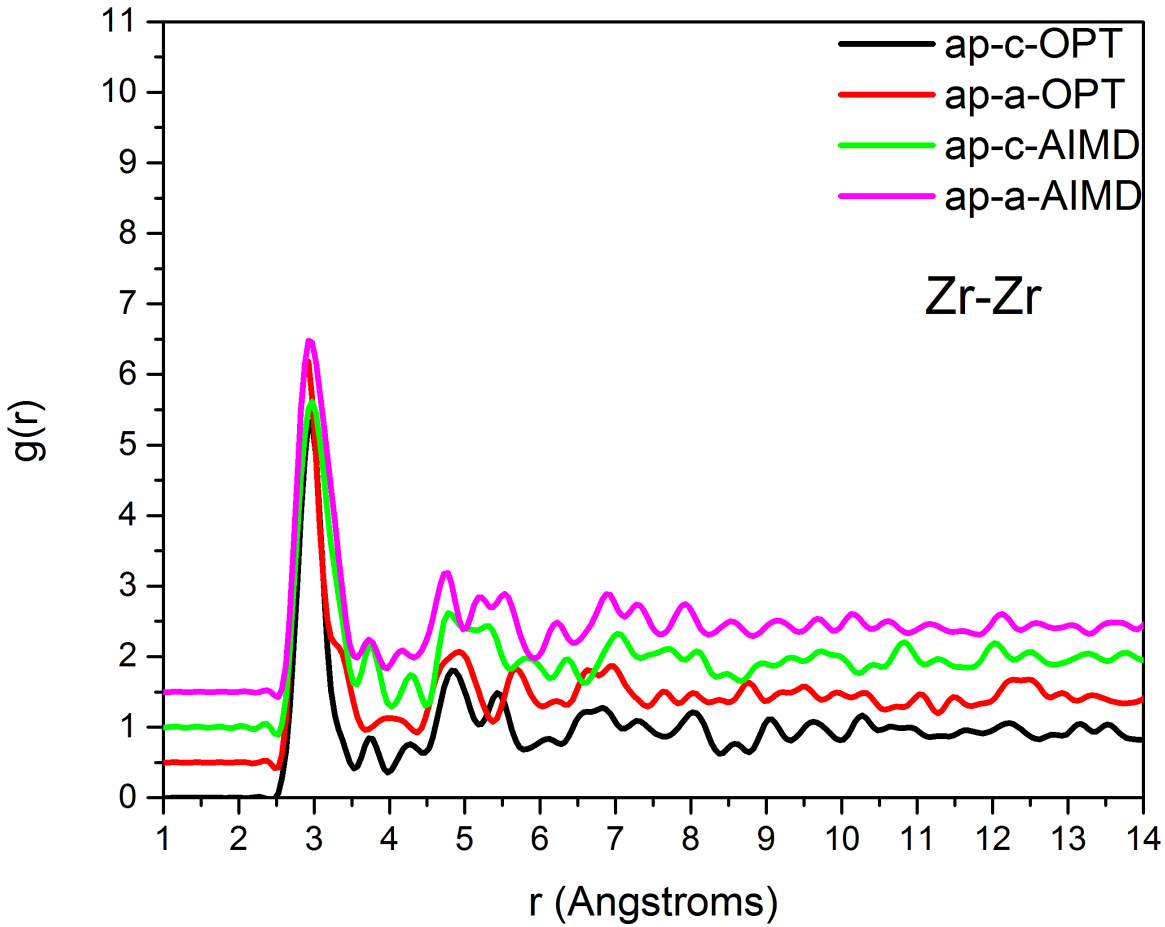

# ap-$Cu_{64}Zr_{36}$ OPT comparison of total PDF

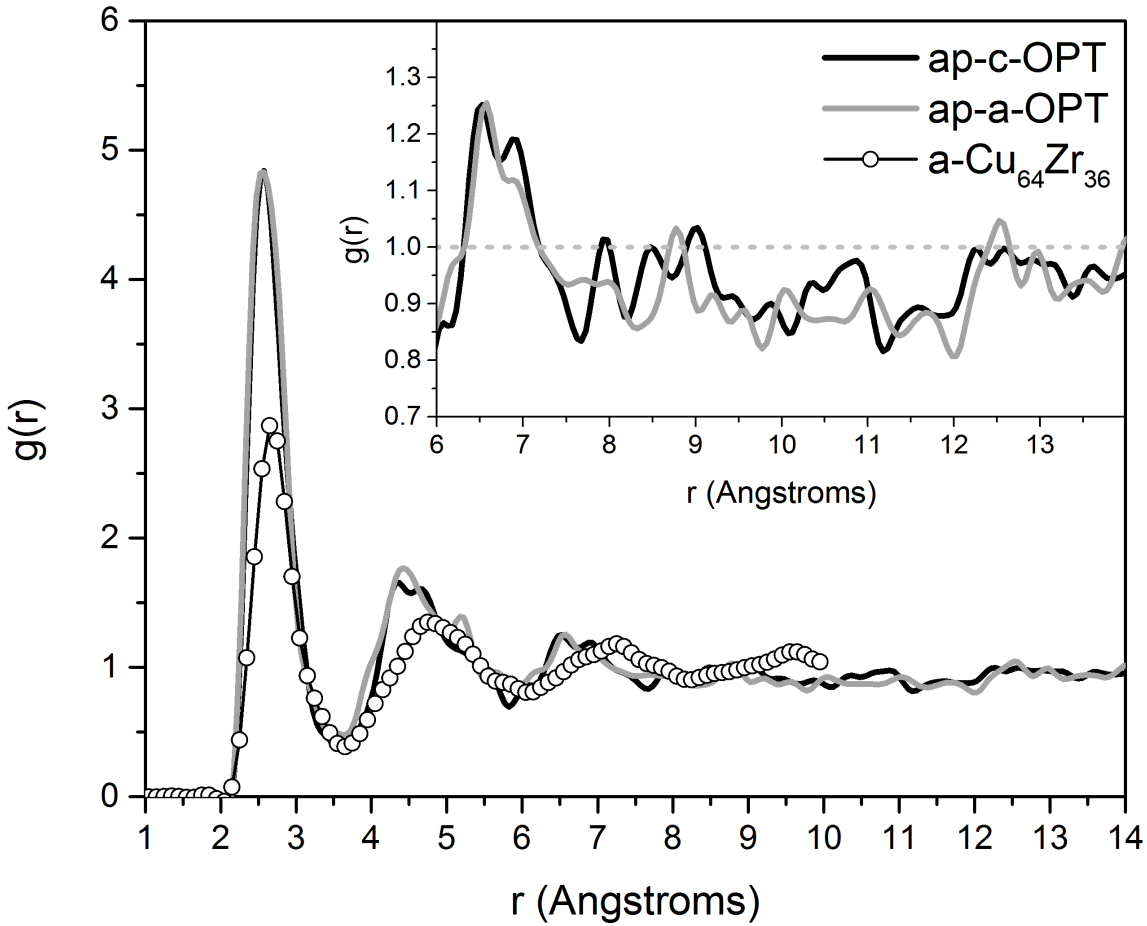

# ap-$Cu_{64}Zr_{36}$ AIMD comparison of total PDF

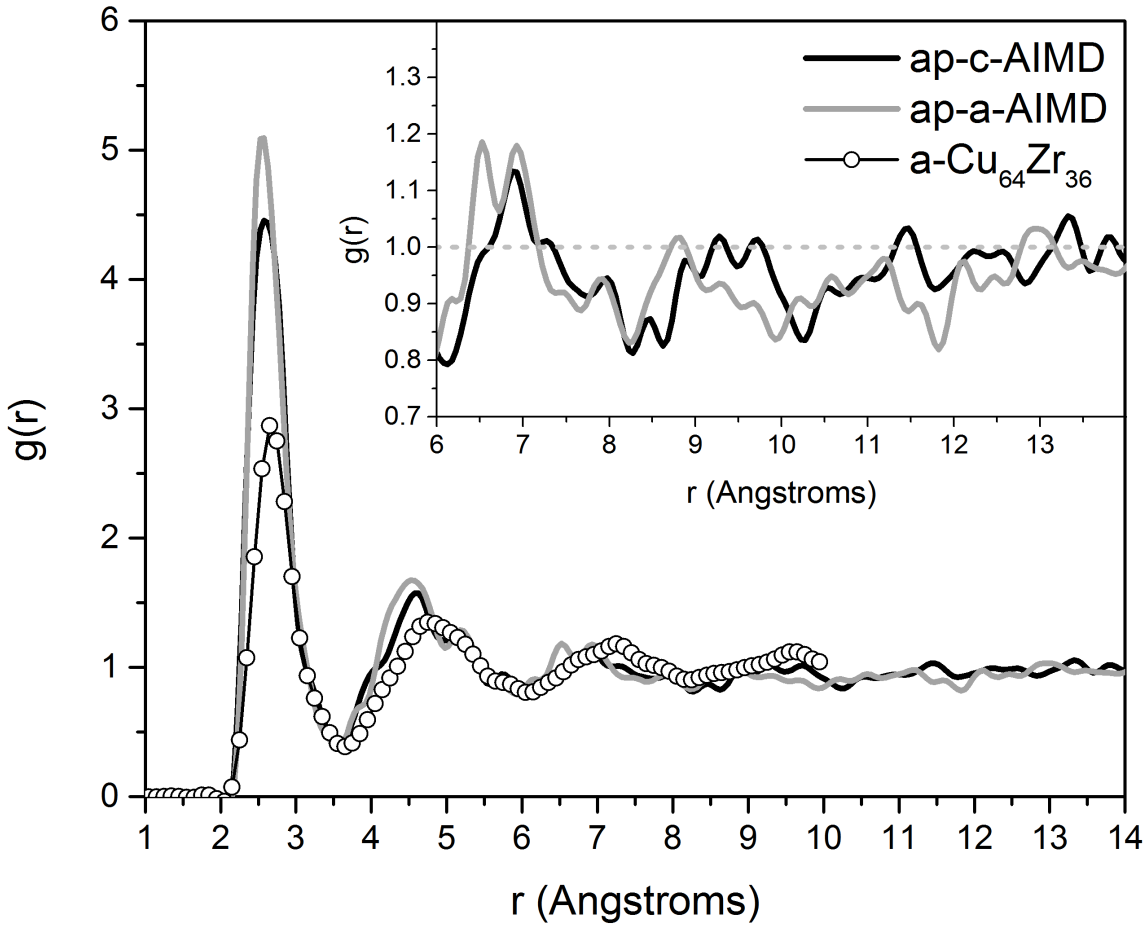

# 1st neighbor positions and coordination numbers

| | $r_{\text{Cu-Cu}}$ | $r_{\text{Cu-Zr}}$ | $r_{\text{Zr-Zr}}$ | $r_{\text{Total}}$ |
|---|---|---|---|---|
| ap-c-OPT | 2.43 | 2.68 | 2.98 | 2.58 |
| ap-a-OPT | 2.43 | 2.73 | 2.93 | 2.58 |
| ap-c-AIMD | 2.43 | 2.73 | 2.98 | 2.58 |
| ap-a-AIMD | 2.48 | 2.68 | 2.93 | 2.58 |
| a-$Cu_{64}Zr_{36}$ | 2.45 | 2.75 | 3.15 | 2.70 |

# 1st neighbor positions and coordination numbers

| | $r_{Cu\text{-}Cu}$ | $r_{Cu\text{-}Zr}$ | $r_{Zr\text{-}Zr}$ | $r_{Total}$ |
|---|---|---|---|---|
| ap-c-OPT | 2.43 | 2.68 | 2.98 | 2.58 |
| ap-a-OPT | 2.43 | 2.73 | 2.93 | 2.58 |
| ap-c-AIMD | 2.43 | 2.73 | 2.98 | 2.58 |
| ap-a-AIMD | 2.48 | 2.68 | 2.93 | 2.58 |
| a-$Cu_{64}Zr_{36}$ | 2.45 | 2.75 | 3.15 | 2.70 |

| | $N_{Cu\text{-}Cu}$ | $N_{Cu\text{-}Zr}$ | $N_{Zr\text{-}Cu}$ | $N_{Zr\text{-}Zr}$ | $N_{Cu}$ | $N_{Zr}$ | $N_{Total}$ |
|---|---|---|---|---|---|---|---|
| ap-c-OPT | 4.5 | 3.8 | 6.7 | 3.7 | 8.3 | 10.4 | 9.0 |
| ap-a-OPT | 4.8 | 3.7 | 6.6 | 3.7 | 8.5 | 10.3 | 9.1 |
| ap-c-AIMD | 4.4 | 3.8 | 6.7 | 4.2 | 8.2 | 10.9 | 9.1 |
| ap-a-AIMD | 4.6 | 3.5 | 6.2 | 4.1 | 8.1 | 10.3 | 8.9 |
| a-$Cu_{64}Zr_{36}$ | 6.7 | 5.3 | 9.4 | 6.3 | 12 | 15.7 | 13.2 |

# ap-$Cu_{64}Zr_{36}$ OPT depletion in total PDF

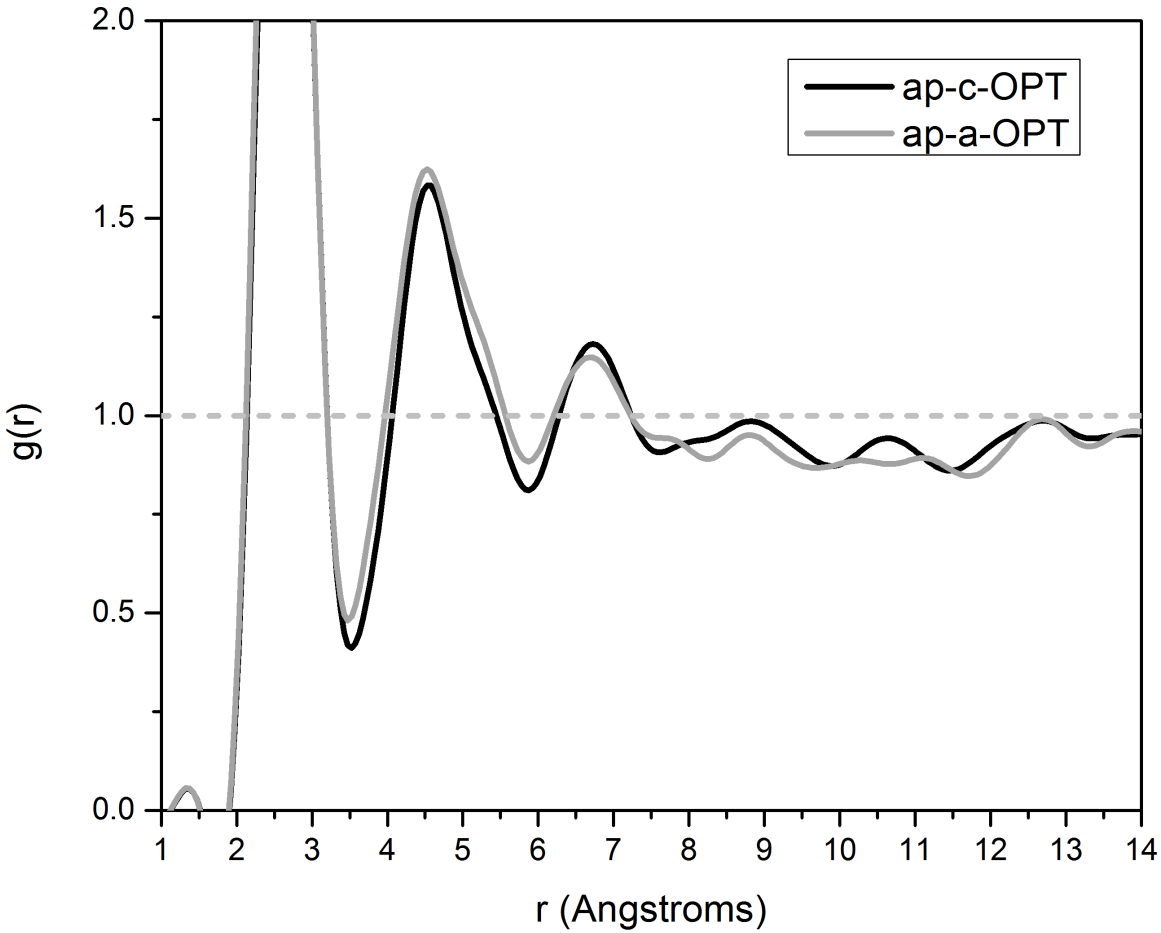

# ap-$Cu_{64}Zr_{36}$ AIMD depletion in toatl PDF

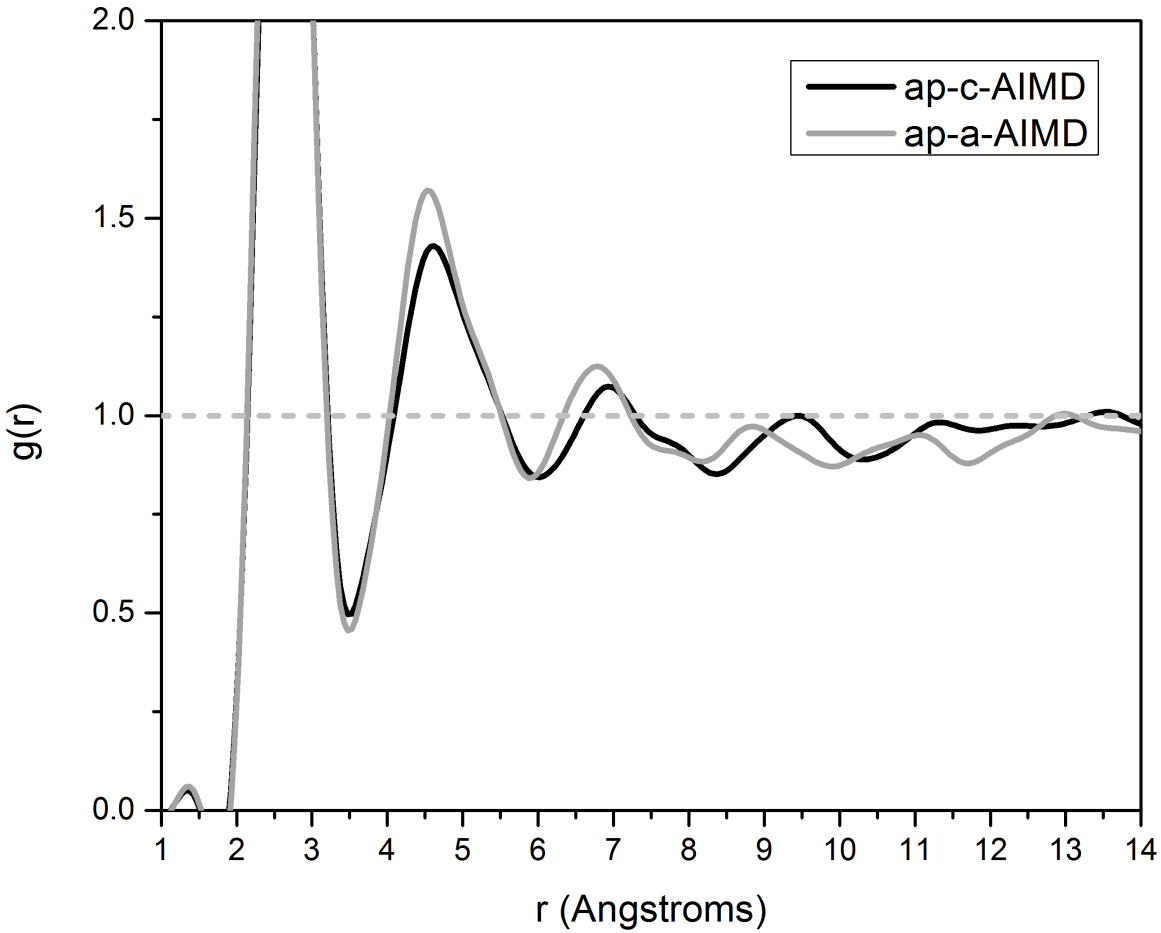

# Pore size estimation

| | Pore size (Å) |
|---|---|
| ap-c-OPT | 7.1 |
| ap-a-OPT | 7.5 |
| ap-c-AIMD | 2.1/3.9 |
| ap-a-AIMD | 5.6 |

# Pore size estimation

| | Pore size (Å) |
|---|---|
| ap-c-OPT | 7.1 |
| ap-a-OPT | 7.5 |
| ap-c-AIMD | 2.1/3.9 |
| ap-a-AIMD | 5.6 |

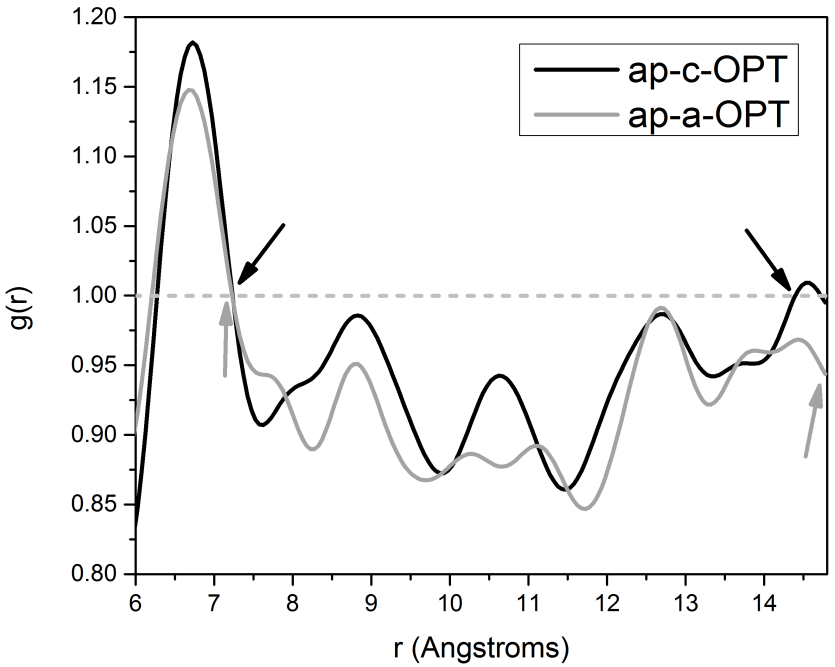

# Pore size estimation

| | Pore size (Å) |
|---|---|
| ap-c-OPT | 7.1 |
| ap-a-OPT | 7.5 |
| ap-c-AIMD | 2.1/3.9 |
| ap-a-AIMD | 5.6 |

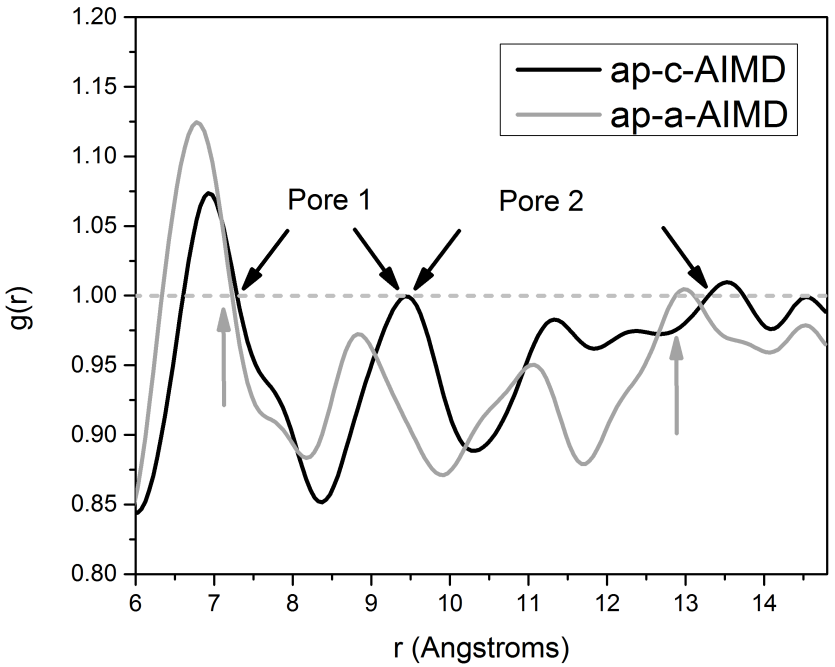

# BAD ap-$Cu_{64}Zr_{36}$ OPT

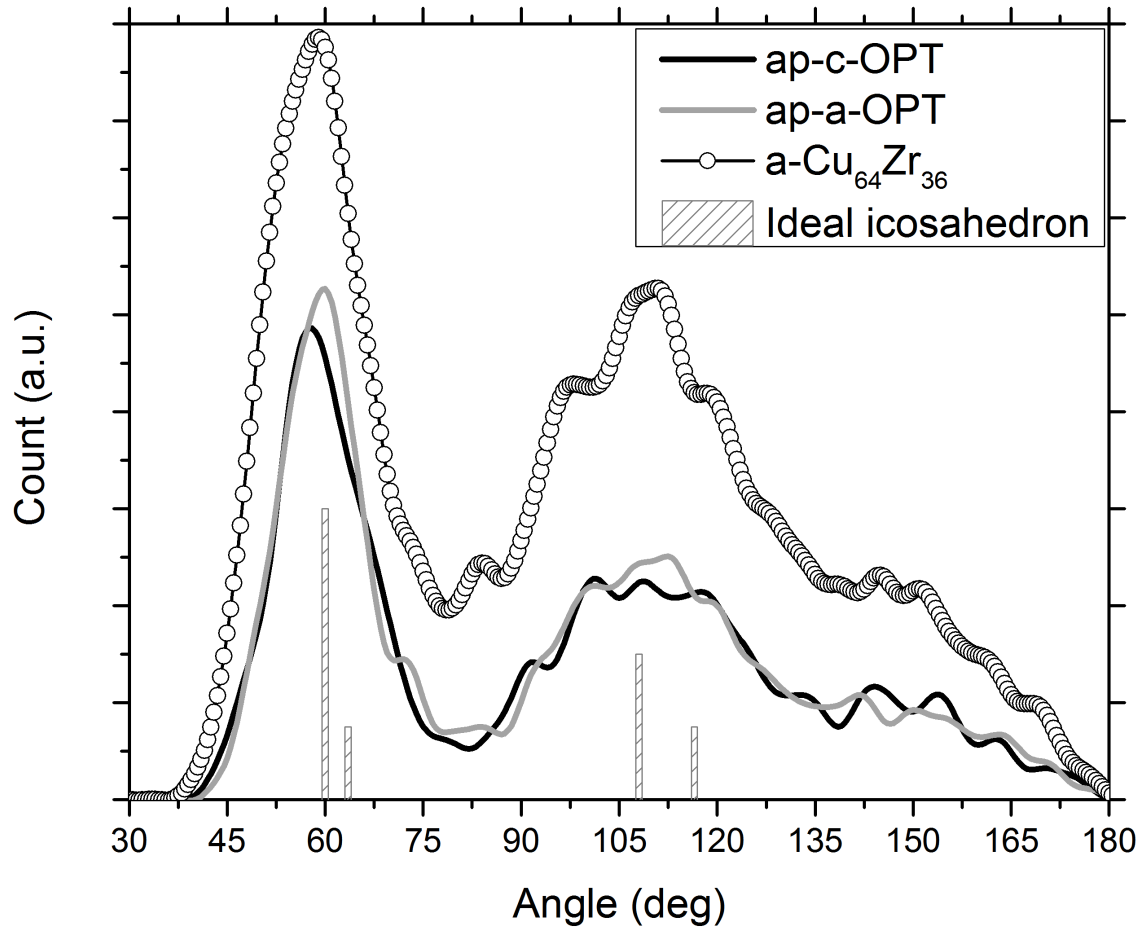

# BAD ap-$Cu_{64}Zr_{36}$ AIMD

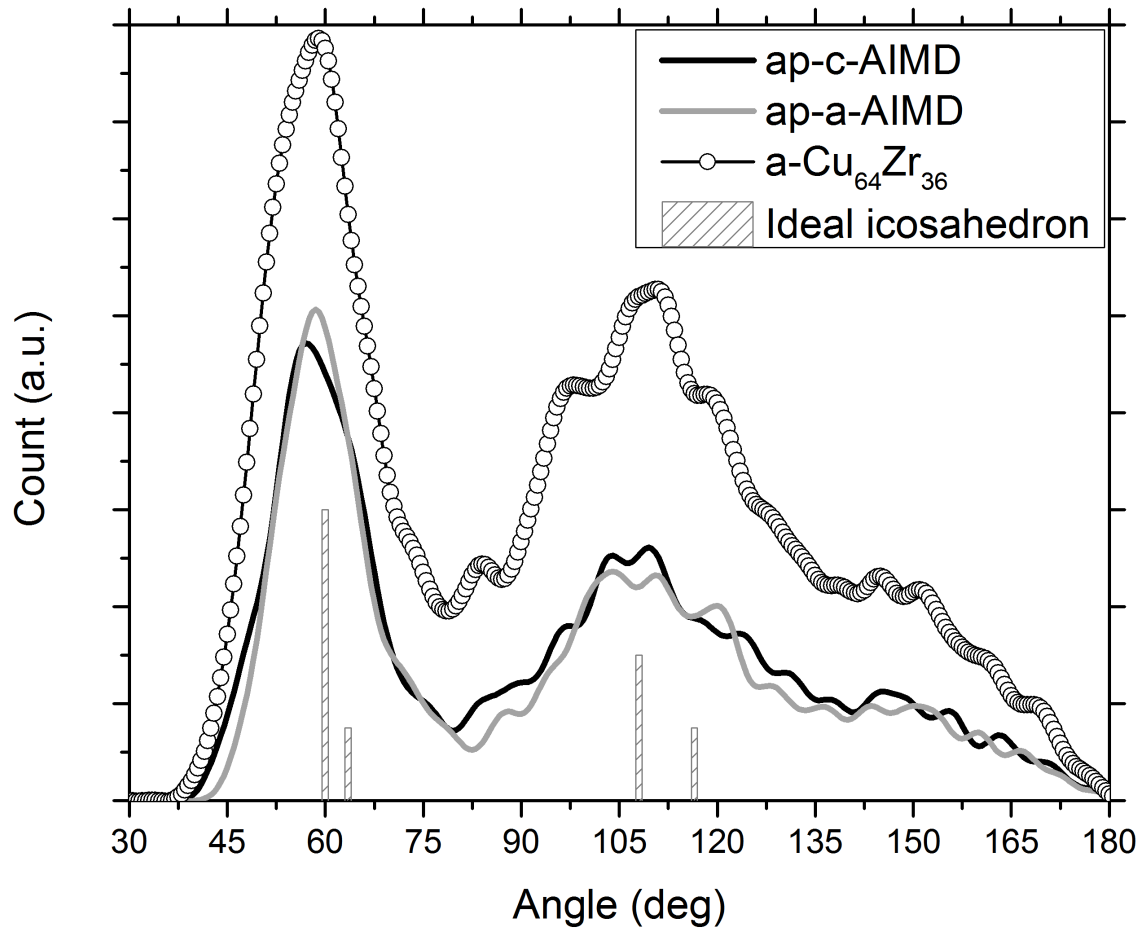

# Conclusions and future development

- We applied the expanding lattice method to obtain nano porous amorphous $Cu_{64}Zr_{36}$ at room temperature by means of *ab initio* molecular dynamics and geometry optimization only.
- The initial amorphous structures became porous whereas the initial crystal cells become both porous and amorphous.
- Larger pores that appeared in simulations with an initial amorphous configuration may be related to a higher energetic cost of disordering initial crystalline structures after EL.
- Low coordination is a consequence of a competition between surface and bulk contributions.
- BAD sharp peak around 60° suggests the existence of distorted Frank-Kasper polyhedra.
- Larger simulation cells would provide insight to verify whether pore topology is cell-size dependent (through and dendritic pores).

# What's next

- Use a larger number of atoms to study pore size and geometry.
- Study other binary and ternary alloys.
- Try different concentrations of Cu-Zr alloy.
- Generate amorphous nanoporous structures with different porosity.
- AIMD at higher temperatures to see its influence in the amorphization process of initial crystalline models.

# Our workgroup

- Prof. Ariel A. Valladares
- Prof. Renela Valladares
- Prof. Alexander Valladares

Students

- Martín Mejía
- Juan Carlos Noyola
- Cristina Romero
- Zaahel Mata
- Sebastián Tamariz
- Jozra Garrido
- Isaías Rodríguez

Former students

- Ph.D. Fernando Álvarez
- Ph.D. Rubén Estrada
- Ph.D. Emilye Rosas
- Ph.D. Ángel Reyes
- Ph.D. Andrés Díaz
- Ph.D. Ulises Santiago

Thank you for your attention!